Synthesis and Potential Adsorption of Fe$_3$O$_4$@C Core-Shell Nanoparticles for to Removal of Pollutants in Aqueous Solutions: A Brief Review

Lima MM[1*], Macuvele DLP[1,2], Muller L[1], Nones J[1], Silva LL[3], Fiori MA[1,3], Soares C[1] and Riella HG[1]

[1]Department of Chemical Engineering, Federal University of Santa Catarina, Florianopolis, SC, Brazil
[2]Department of Chemistry, Pedagogical University of Mozambique, Branch of Niassa, Mozambique
[3]Post-Graduation Program in Environmental Science and Post-Graduation Program in Technology and Management of the Innovation, Community University of Region Chapeco, Chapeco, SC, Brazil

Abstract

Core-shell Fe$_3$O$_4$@C nanoparticles consist of a magnetic core and carbon coating, and exhibit high adsorptive capacity, easy magnetic separation and reusability. Due to these properties, core–shell Fe$_3$O$_4$@C nanoparticles have great potential application in adsorption, separation and wastewater treatment. Magnetic separation based on the super paramagnetic Fe$_3$O$_4$ has received considerable attention and is widely used for the removal of dye, oil pharmaceuticals and metals from water due to its high efficiency and economic viability. Therefore, the main characteristics of the core-shell Fe$_3$O$_4$@C nanoparticles, the different types of synthesis, as well as the main applications for the removal of water pollutants were reviewed. In this brief review, an overview of the basic properties of the Fe$_3$O$_4$@C core-shell nanoparticles are given, and the most important and more frequently used methods for the synthesis of Fe$_3$O$_4$@C core-shell nanoparticles have been summarized along with the description of its adsorbent application potential.

Highlights

- Magnetic core-shell Fe$_3$O$_4$@C nanoparticles combine excellent adsorptive capacity and easy magnetic separation.
- Core-shell nanoparticles show high regeneration capability.
- The use of magnetic core-shell Fe$_3$O$_4$@C nanoparticles provides over 90% removal of pollutants in aqueous media.
- Magnetic core-shell Fe$_3$O$_4$@C nanoparticles regeneration has been manifesting great potential in water treatment.

Introduction

Several industries such as fertilizer, paper, pharmaceutical, plastic and textile consume in their processes large amounts of water, and consequently dispose considerable volumes of pollutants daily, such as dyes, heavy metals, pharmaceuticals, among others.

Industrial processes use dyes and substantial volumes of water to dye products such as tissue, leather, paper and plastics. Such procedures generate a large amount of dye that is released into natural waterways [1], risking to reduce sunlight penetration and deplete the dissolved oxygen, not to mention the production of some toxic, mutagenic and carcinogenic intermediates by different reaction such as hydrolysis and oxidation of dye [2].

The pollution produced by pharmaceutical products in surface and ground waters has been acknowledged by many countries as an environmental issue, leading the pharmaceutical industry to use the designation Active Pharmaceutical Ingredients to describe products that are pharmacologically active, resistant to degradation, highly persistent in aqueous medium, and potentially able to produce adverse events in water organisms and have a negative impact on human health [3]. Among pharmaceuticals, antibiotics have received particular attention since the late 90s [4] due to correlations between the development and rapid expansion of antibiotic resistance and their total consumption and occurrence in the environment [4,5].

Furthermore, another serious environmental problem is pollution by heavy metals [6], which are persistent, non-biodegradable, toxic and bio accumulative in the aquatic ecosystem [7]. This pollutant generally enters the aquatic environment through atmospheric deposition, erosion of geological matrix or deriving from anthropogenic activities caused by industrial discharges, domestic sewage and mining wastes [8]. After their introduction into the aquatic ecosystem, most metals are attached to fine-grained particulates and, as a result of settling, accumulate in bottom sediments, where they may cause adverse biological effects even when water quality criteria are not exceeded [7].

With this in mind, several technologies have been developed to remove water pollutants, such as biological treatment processes, chemical oxidation processes, membrane separation and ion exchange processes and adsorptions processes [9-11]. Among these processes the adsorption technology is regarded as one of the most competitive due to its wide application scope, excellent efficiency of water treatment and its high capacity to recover valuable products and raw materials.

Thus, continuous efforts are being made to synthesize adsorbents with excellent performance, which require a good adsorption capability and convenient recovery from aqueous media [12,13].

In general, these adsorbents have a functional surface or hierarchical porous structure with high specific surface area, and exhibit excellent dye adsorption performance [1]. Traditional adsorbents, such as activated carbon, silica, zeolites, peat and chitin are limited as they cannot meet the growing industrial demand on account of their limited adsorption capacity and slow recovery process [13]. In addition, traditional

separation methods of adsorbents in water, including centrifugation and filtration, are time consuming and lead to relatively high costs.

In recent years, a great deal of active research has been performed on novel adsorbents, exploring various configurations of adsorbents to maximize their adsorptive capacity, particularly by incorporating nanoparticles. The unique advantages of nanoparticles are their small size, large surface area and the quantum size effect, which theoretically increases the adsorption capacity for nanoparticle adsorbents [14].

Therefore, Fe$_3$O$_4$-based magnetic nano adsorbents have drawn considerable attention due to their simple and fast separation properties under an external magnetic field [1]. Furthermore, magnetic adsorbents have distinct advantages such as selective absorptivity, easy recovery, strong magnetic responsiveness and favorable water dispersibility. Characteristics such as a good regeneration capability substantiate the great potential of Fe$_3$O$_4$@C in water treatment [15-17].

In this brief review, an overview on the basic properties of the methods of the most important and frequently used synthesis of Fe$_3$O$_4$@C core-shell nanoparticles has been summarized along with the description of its properties and application as an adsorbent.
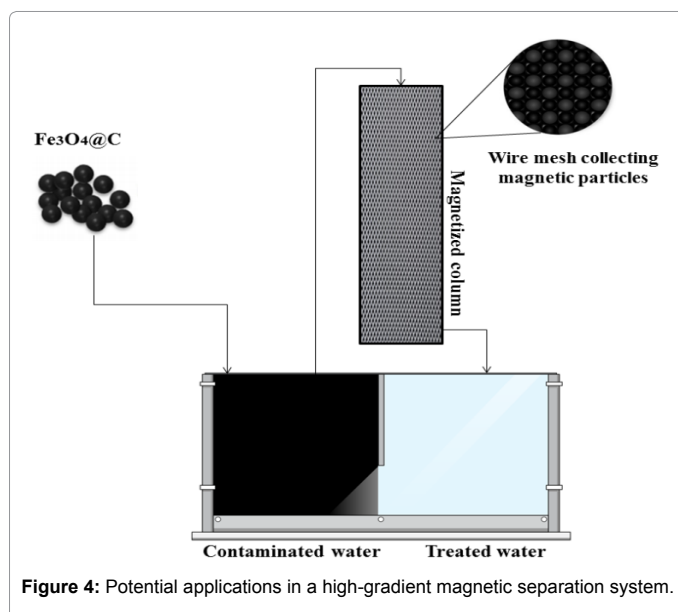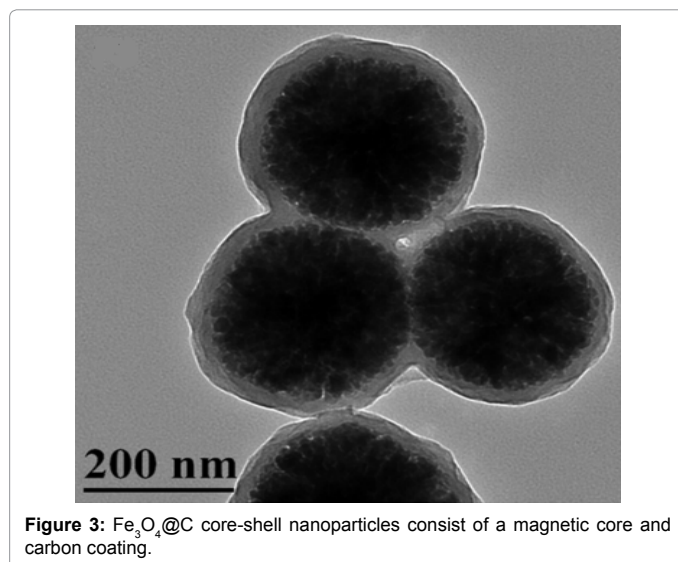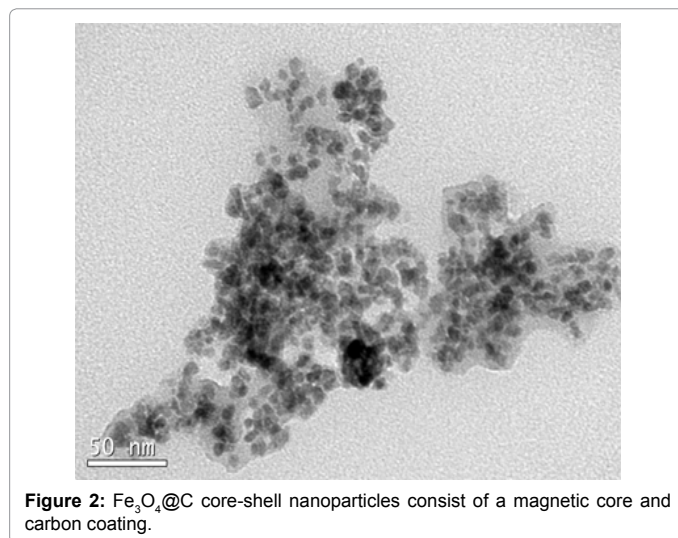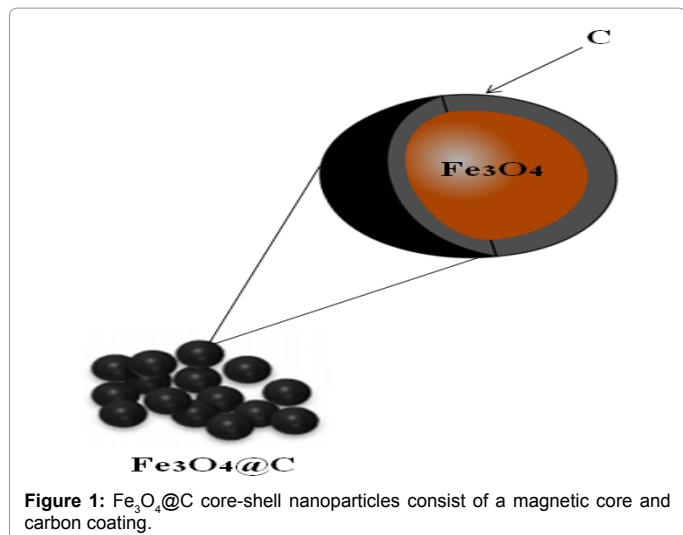
Fe$_3$O$_4$@C core-shell nanoparticles characteristics

Fe$_3$O$_4$@C core-shell nanoparticles consist of a magnetic core and carbon coating (Figures 1-3), owing its importance to characteristics such as high adsorption, easy magnetic separation and regeneration capacity [12,15-24].

These structures are being used in many fields such as magnetic resonance imaging, medicine, biology, immunoassay, drug delivery and separation methods [25,26]. This widespread application is due to their useful properties including small size, high specific surface area, biocompatibility, high saturation magnetization level, low toxicity and injectability in industrial systems [27].

Studies show that, depending on the synthesis condition, it is possible to obtain ferromagnetic Fe$_3$O$_4$@C core-shell nanoparticles [28,29] or super paramagnetic [15,30,31]. These characteristics depend on the phases of iron oxide used, which can be magnetite (Fe$_3$O$_4$) [29,32-34], hematite (α-Fe$_2$O$_3$) [35-37], maghemite (γ-Fe$_2$O$_3$) [38-40] and wustite (FeO) [41].

Among the advantages found in theses nanoparticles, one that stands out is its easy separation, which is related to its magnetic behavior, with

Figure 2: Fe$_3$O$_4$@C core-shell nanoparticles consist of a magnetic core and carbon coating.

Figure 3: Fe$_3$O$_4$@C core-shell nanoparticles consist of a magnetic core and carbon coating.

Figure 1: Fe$_3$O$_4$@C core-shell nanoparticles consist of a magnetic core and carbon coating.

Figure 4: Potential applications in a high-gradient magnetic separation system.

potential applications in a high-gradient magnetic separation system, as illustrated in Figure 4. This system starts with the addition of nano adsorbents to the contaminated water tank, with resulting pollutant adsorption by the nanoparticles. After a certain time, the separation stage, in which the water passes through a column containing a magnetized grid begins, and magnetic nano adsorbents are attracted by the magnetic field and retained in the grid. The water, now free of pollutant, passes to the second tank, concluding the adsorption process. The nanoparticles can then be recovered by desorption. The industrial usage of magnetic water treatment can be traced back to more than 100 years. Faunae and Cabell invented an electromagnetic device to treat boiler feed water [42], and Hay [43] received the first United States patent for a water treatment device that employed a magnetic field.

Magnetic separation based on the Fe$_3$O$_4$ has received considerable attention and is widely used in wastewater treatment mainly due to its low cost and high efficiency [13]. In such separation processes, the interaction of magnetic forces and other forces is important to control and direct the particle movement. Depending on the magnitude of the acting magnetic force, the whole separation process can be influenced by specific movements or magnetically induced agglomeration of the magnetic particles [44].

Several works in the literature show the magnetic separation capacity of Fe$_3$O$_4$@C core-shell nanoparticles and their application in various effluent treatments [12,17-24]. Wu et al. [17] stated in their study that easy separation is the major priority of magnetic adsorbents. The authors demonstrate the easy magnetic separation of Fe$_3$O$_4$@C after the adsorption of methylene blue (MB). Hao et al. [19] studied the magnetic separation of Fe$_2$O$_3$@C nanoparticles after dye removal. They observed that the dye-loaded in iron oxide/carbon nanoparticles could be easily separated by placing a conventional laboratory magnet beside the glass bottle.

On the other hand, the magnetism of Fe$_3$O$_4$@C nanoparticles can be decreased by a carbon coating. Shouhu et al. [45] prepared carbon-encapsulated magnetic nanoparticles and observed that the products exhibited typical ferromagnetic magnetic curves, with a saturation magnetization much lower than that of the corresponding bulk Fe$_3$O$_4$. This can occur due to the amorphous carbon shell in the disordered structure at interfaces providing less magnetic moment per mass unit than that of ferromagnetic core regions. However, several researchers such as Kakavandi et al. [32] affirmed that this magnetic composite could be applied as a catalyst for environmental purposes, being subsequently easily and rapidly removed from the solution without leaving residues.

Another advantage Fe$_3$O$_4$@C core-shell nanoparticles is its easy regeneration. Lin et al. [12] affirmed that the stability and regeneration ability of the adsorbents are crucial for its practical applications. The removal of contaminants from wastewater by adsorption implicates a reduction of operation costs. The cost of their disposal or regeneration determines the feasibility of applying the adsorbent systems in large-scale operations. Lin et al. [12] observed in their studies that Fe$_3$O$_4$@C nanoparticles with mesoporous carbon, after five adsorption-desorption cycles, still demonstrated good stability capacity. On the other hand, Wu et al. [6] observed that the recycling of Fe$_3$O$_4$@C led to a decrease of adsorption capacity. After the first recycle, the relative capacity was 96.3%, decreasing to 59% at the fourth cycle. The results indicated that Fe$_3$O$_4$@C nanoparticles could be regenerated during the applications, but in such cases its adsorptive capacity decreases. Kakavandi et al. [32], who observed that Fe$_3$O$_4$@C retained its stability and adsorptive

activity even after several cycles, which could significantly reduce the operation costs in practical applications.

Synthesis of Fe$_3$O$_4$@C core-shell nanoparticles

Core-shell has attracted considerable attention due to its well-ordered assembly structures that are synthesized through chemical bonding or other forms of interaction between carbon and iron [46]. Depending on the synthesis techniques, a variety of scales and shapes can be synthesized, such as sphere, cube, prism, platelets, wire, rod, tube, etc. In order to synthesize Fe$_3$O$_4$@C core-shell nanostructures at different scales and shapes, several methodologies have been developed [34,37,47-55].

According Cunningham and Burgi [56], nano materials synthesize methods can be divided in two categories (Figure 5).

Top-down: a process that starts from a bigger particle to obtain a smaller one through the application of externally controlled tools to cut, grind and shape materials in the desired form and scale [57]. The most common techniques are lithographic [58], laser processing [59] and mechanic ones [60].

Bottom-up: approach involves the fabrication of structures from smaller units, using the properties that they possess to induce their self-assembly in the desired manner [56]. The particle is constructed atom by atom until reaching the desired size [57]. The most common techniques are vapour chemical decomposition [61], laser induced assembly [62], self-assembly [63], colloidal aggregation, film deposition and growth [64] and chemical synthesis.

Both top-down and bottom-up have advantages and disadvantages, but compared to top-down methods the bottom-up self-assembly approach is cheap and enables the manufacturing of two-dimensional or three-dimensional samples with a large area, making it attractive for several applications [56]. Furthermore, bottom-up stands out due to its capacity to produce significantly smaller particles with greater precision, greater process control and minimal energy loss. This process is the ideal for the synthesis of core-shell nanoparticles due to the bigger process control during the synthesis, thus achieving a uniform coating of the core during particle formation, along with the aforementioned advantages [57].

According to Laurent et al. [65], the coating of iron oxides, e.g., magnetite, can not only protect the core, but also promotes the increase
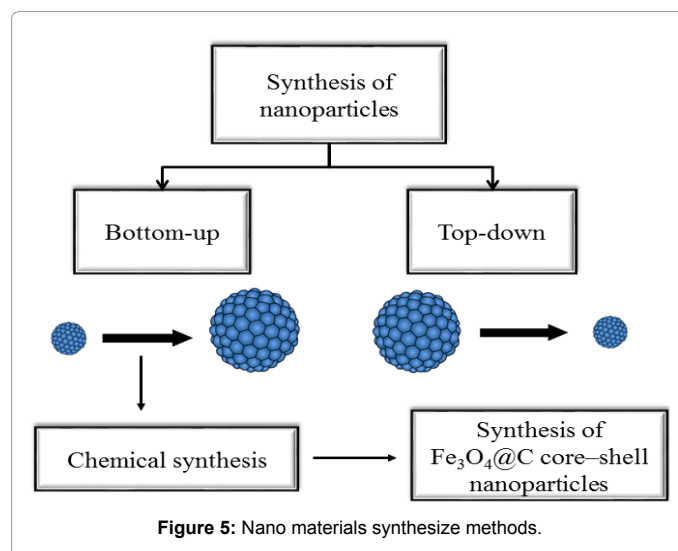

Figure 5: Nano materials synthesize methods.

in nanoparticle stability. Therefore, there are several studies addressing the use of different coating materials for magnetic nanoparticles, such as silicon [66], polyanile [67], chitosan [68], carbon [35,52,53,55], among others. A comparison between silicone and carbon as a coating material for metallic particles shows that carbon presents a much greater stability in various types of environments and conditions, both for acid and basic media, and high temperatures and pressure [34].

Several different methodologies are found in the literature for the synthesis of core-shell Fe$_3$O$_4$@C nanoparticles, such as solvothermal [49], chemical vapour decomposition [48], hydrothermal coprecipitation [34], pyrolysis [55,53], combustion waves [69] and synthesis by microwave [55], as well as the combination of two or more methods.

Hydrothermal coprecipitation

The most common and most efficient method for the synthesis of core-shell Fe$_3$O$_4$@C nanoparticles is hydrothermal coprecipitation, which consists of a precipitation stage of the oxide in alkali medium followed by a carbon coating [34] (Figure 6).

A hydrothermal process is one which involves reactions in aqueous solvents at high temperatures and vapour pressures, utilizing sealed containers such as autoclaves and pressure tubes [70]. In contrast, coprecipitation processes occur when there is a reaction between two or more hydro soluble salts and the formation of at least one insoluble salt that precipitates [57,71]. Thus, in the hydrothermal coprecipitation process there is the combination of these two methods for the formation of both the core, by the precipitation of Fe$_3$O$_4$, and the carbon shell, by the hydrothermal process.

The coprecipitation process occurs in two stages: first, a fast nucleation period, which happens when the concentration of the reagent reaches critic super saturation; afterwards, there is the stage for the slow growth of the cores by the diffusion of solutes on the crystal's surface [57,65,71]. The formation of the shell in the core occurs through a heterogeneous nucleation process. The particles in the shell material are directly deposited on the core's surface and continue the process of the core formation and growth on its surface, instead of forming new cores at the bulk phase [57].

Xuan et al. [34] performed the synthesis of Fe$_3$O$_4$@C in a single step by hydrothermal coprecipitation. The authors affirmed that the use of this synthesis route allowed the attainment of uniform and stable core-shell nanoparticles in a fast and uniform way. The authors stated that the formation of Fe$_3$O$_4$@C occurred in this manner: Fe$_3$O$_4$ nanoparticles were formed by the reduction of Fe^{3+} by glucose in alkaline conditions from the decomposition of urea. The magnetic particles formed in the solution possess a reactive surface which, after the carbonation of glucose, bond with carbon, forming the shell of the Fe$_3$O$_4$ particle. The authors concluded that, compared to other methods for the formation of magnetic metal @C structures, the one-step carbonization reaction here is conducted at a relatively low temperature (180°C). Bhattacharya et al. [41] applied the same technique of synthesis of Fe$_3$O$_4$@C core-shell nanoparticles used by Xuan et al. [34], adding, however, poly-ethylene glycol (PEG) as a chemical stabilizer to prevent nanoparticles agglomeration. Thus, the authors produced spherical nanoparticles with a uniform size distribution.

During the synthesis of nanoparticles, factors such as pH, temperature, the nature of salts (perchlorides, chlorides, sulphates and nitrates) and the ratio of Fe^{2+}/Fe^{3+} concentration can be adjusted to control format, size, magnetic characteristics and surface properties

[57,65,71,72]. Furthermore, the use of surfactant agents can help control the dispersion of the magnetic nanoparticles, reducing the formation of agglomerates through the stabilization of attractive and repulsive forces [41,65].

In addition to the synthesis strategies described above, researches have recently emerged in the literature focusing on obtaining nanoparticles with spheres, chains and rings controlled by reaction parameters [72]. For instance, Li et al. [72], reported for the first time the selected-control, large scale synthesis of mono dispersed Fe$_3$O$_4$@C core–shell spheres, chains, and rings with tunable magnetic properties based on structural evolution from eccentric Fe$_2$O$_3$@poly acrylic acid (PAA) core-shell nanoparticles. The method basically consists of producing Fe$_2$O$_3$ nanoparticles via hydrothermal reaction at a high temperature, followed by the mixing of nanoparticles with PAA to form Fe$_2$O$_3$-PAA. Finally, to obtain Fe$_3$O$_4$@C core-shell spheres, Fe$_2$O$_3$-polymer is heated under an inert atmosphere. Then mono dispersed Fe$_3$O$_4$@C core-shell spheres and rings were fabricated in a controlled way by structural evolution from eccentric Fe$_2$O$_3$@PAA core-shell NPs as starting materials by heat treatment at 400°C for 3 h, 600°C for 5 h, and 600°C for 7 h, respectively, in argon atmosphere. When the eccentric Fe$_2$O$_3$@PAA core–shell NPs were treated at 600°C for 5 h, Fe$_3$O$_4$@C core–shell particle chains were obtained. When the treatment time was prolonged to 7 h, the products were ring-like Fe$_3$O$_4$@C core-shell structures. Figure 7 shows a representative TEM image of the 1D particle chains. The authors believe that the formation of the anisotropic structure is due to magnetic dipolar interaction between the magnetic NPs, which favors a head-to-tail orientation [72]. However, the morphology of the nanoparticles remains spherical even with the temperature and time variation in the Fe$_2$O$_3$@PAA treatment, although the increase in temperature favored the formation of particles with larger size, about 1 μm [72]. Similar methodology was applied by Wang et al. [53], with a major difference in the initial stage, since in this work the authors produced nanoparticles of Fe$_3$O$_4$ instead of Fe$_2$O$_3$. Nonetheless, the subsequent steps were substantially similar. Besides its excellent mono dispersity, uniform diameter, and high magnetic saturation, the product had a good hydro philicity due to the existence of remnant oxygen-containing groups [53].

Wang et al. [73] synthesized carbon encapsulated magnetic nanoparticles by heating an aqueous glucose solution containing Fe@ Au (Au coated Fe nanoparticles) or Ni nanoparticles at 160°C for 2 h. They concluded that, by using this method, it was possible to obtain nanoparticles with uniform Fe/Au soaked carbon spheres with an average particle size of 200 nm. Recently, Fe$_3$O$_4$@C core-shell has been developed at room temperature by applying a hydrothermal process consisting of three steps: at first, hematite (α-Fe$_2$O$_3$) nano rods were obtained; α-Fe$_2$O$_3$@C core-shell nano rods were subsequently fabricated using glucose as a carbon source by a hydrothermal method; finally, Fe$_3$O$_4$@C core–shell were synthesized after an annealing treatment of the product from the previous stage under a flow of a Ar/H$_2$ mixture
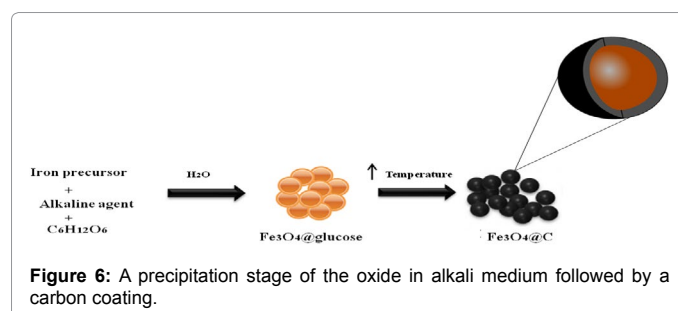

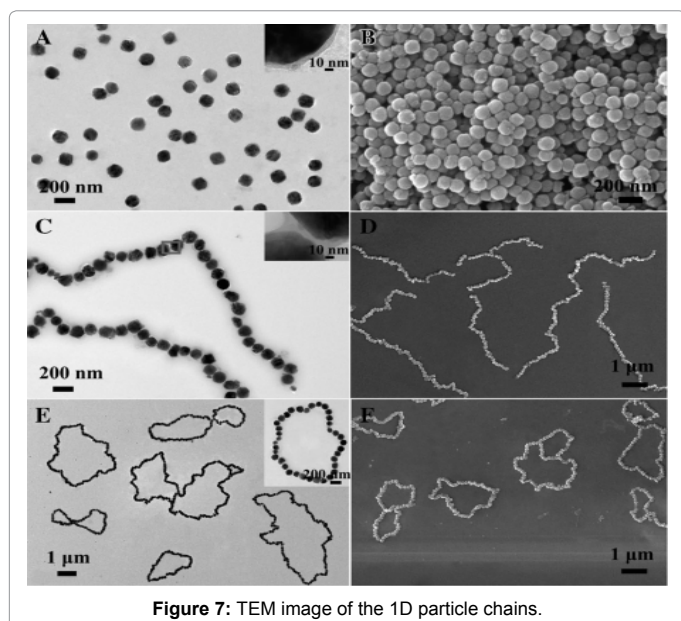**Figure 6:** A precipitation stage of the oxide in alkali medium followed by a carbon coating.
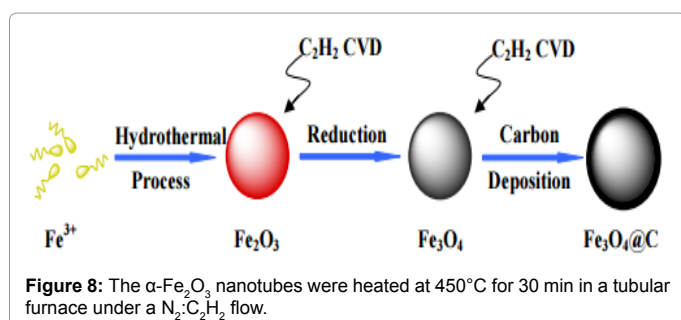
Figure 7: TEM image of the 1D particle chains.

Figure 8: The α-Fe$_2$O$_3$ nanotubes were heated at 450°C for 30 min in a tubular furnace under a N$_2$:C$_2$H$_2$ flow.
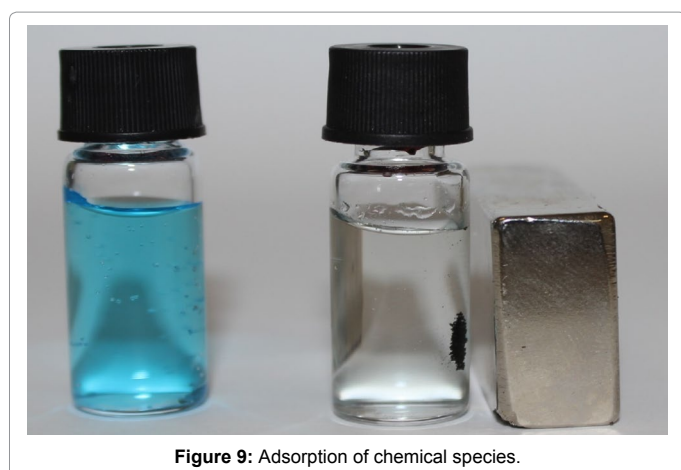

Figure 9: Adsorption of chemical species.

[37]. Iinterestingly, Fe$_3$O$_4$ core has shown many pores whose mean diameter is about 12 nm and its shell exhibits an enhanced degree of graphitization [37].

Solvothermal method

Solvothermal synthesis is a method for preparing a variety of materials such as metals, semiconductors, ceramics, and polymers. The process involves the use of a solvent under moderate to high pressure (typically between 1 atm and 10,000 atm) and temperature (typically between 100°C and 1000°C), which facilitate the interaction of the precursors during synthesis. The method can be used to prepare thermodynamically stable and metastable states, including novel materials that cannot be easily formed by other synthetic routes [74].

Zheng et al. [49] described a simple one-step solvothermal synthesis of Fe$_3$O$_4$@C using glucose, FeCl$_3$·6H$_2$O, CO(NH$_2$)$_2$ and ethylene glycol (EG) as raw materials. The nanoparticles produced are constituted by aggregates composed mainly of nano crystals with sizes between 10-12 nm and possessing hollow interior, high magnetization, excellent absorption properties and abundant surface hydroxyl groups. The role of glucose in this synthesis, apart from being a carbon source, is also to control the size of the resulting nanoparticles, i.e., the higher the glucose concentration the smaller the size of the resulting nanoparticles. The authors believe that the adsorption of carbon on the surface of the nano metric magnetite prevents the subsequent aggregation of particles, consequently resulting in a smaller size. On the other hand, it can decrease the surface tension between the crystallization phase and the surrounding solution, resulting in an increase of the nucleation rate [49].

Furthermore, Fe$_3$O$_4$@C was successfully synthesized by combining solvothermal, polymerization and high temperature carbonization. The magnetic Fe$_3$O$_4$ nanoparticles with a diameter of ~250 nm have been synthesized by the solvothermal method [75]. The authors also studied the effect of resorcinol-formaldehyde (RF) concentration on the size and thickness of RF shell. By adjusting the concentration of the RF precursor in the reaction solution, the thickness of RF shell can be adjusted in the range of 50~150 nm [75]. However, the effect on the thickness of the RF shell on Fe$_3$O$_4$@C particle size after carbonization was not investigated, but would have been interesting to do so, since the aim of the work was to produce Fe$_3$O$_4$@C core-shell.

Recently, Fe$_3$O$_4$@C MNCPs were prepared by the reduction of ferrocene via a solvothermal reaction. The Fe$_3$O$_4$@C MNCPs in a nano-scale diameter were used as building blocks in the self-assembly of the photonic crystal with a three-dimensional structure [76]. Effects of three important parameters, including temperature, dispersion concentration and solvent type on evaporation-induced self-assembly have been investigated. These factors have been proven to have a significant impact on structural regularity and lustrousness of the resulting photonic crystals. Meanwhile, photonic crystals with different diffraction colors were obtained by controlling particle size of MNCPs through adjusting solvothermal reaction temperature [76].

Chemical Vapor Deposition (CVD)

CVD is a quite interesting synthetic route core-shell from an environmental point of view; it does not use any solvent. Another advantage of this method is the possibility of also producing core-multishell, making this technique quite versatile [77]. Basically, the surface of the core-particles is used for the heterogeneous nucleation of the solid shell phase. Similarly to the gas phase synthesis, whether a precursor will react and form particles in the surrounding liquid phase by homogeneous nucleation or directly react on the core particle surfaces by chemical deposition depends on the processing conditions [78].

For instance, Wang et al. [79] synthesized Fe$_3$O$_4$@C core-shell via CVD route, but the initial oxidation was carried out by hydrothermal synthesis. The process basically consisted of heating the material to a temperature of 550°C in a horizontal tube furnace under an Ar atmosphere and subsequently introducing the carbon source (acetylene) into the reactor, obtaining the final product after 15 minutes. The XRD results show that the Fe$_2$O$_3$ spheres with a diameter of 400 nm were completely converted to Fe$_3$O$_4$ after the CVD process. SEM, EDS and

TEM results show that a thin carbon layer with a thickness of ~10 nm was formed on the surface of the Fe$_3$O$_4$ particles [79].

Fe$_3$O$_4$@C with a core–shell tubular structure was synthesized by CVD route by Zhu et al. [80]. The α-Fe$_2$O$_3$ nanotubes were heated at 450°C for 30 min in a tubular furnace under a N$_2$:C$_2$H$_2$ flow (Figure 8). The volume ratio of N$_2$ to C$_2$H$_2$ was 9:1 and the total gas flow rate was 100 mL·min^{-1} After the CVD reactions, C-Fe$_3$O$_4$-C nanotubes with a core–shell structure were obtained [81]. Similarly Wang et al. [82] synthesized Fe$_3$O$_4$@C core-shell using the same methodology as Zhu et al. [81], having obtained core-shell nanoparticles with a carbon layer between 3-5 nm. Additionally, the same authors observed the formation of carbides with an extended time of the deposition reaction.

It is important to note that CVD is not only a solvent-free method, but also extremely practical, since it requires little time (15-30 minutes) for the formation of the core-shell structure when compared to the hydrothermal route. The time depends on the conditions of the CVD process such as: initial morphology of the precursor oxides, temperature, and acetylene flow different carbon layer sizes can be obtained. Another factor worth highlighting is the CVD process time. For instance, for times greater than 20 minutes carbide formation occurs [82].

Combustion waves

The method that uses combustion waves in the synthesis of core-shell-like structures was developed in the southern belt by researchers from the University of Correia [69]. This process consists of initially producing the hybrid composite of Fe$_2$O$_3$ nanoparticles and nitrocellulose via wet impregnation, then combustion waves are generated by a tungsten resistance promoting the reduction of the carbon and consequent conversion of Fe$_2$O$_3$ to Fe$_3$O$_4$, thereby forming the nanostructured Fe$_3$O$_4$@C core-shell [69].

This simple one-pot transformation by combustion waves in hybrid composites of chemical fuels and core materials could be applied to the transformation of other metal oxides and the synthesis of ceramics, as well as providing a general strategy for the formation of a carbon coating layer on nanostructured materials. This reaction is completed within a few seconds without a costly setup, since it is performed in open-air conditions [69]. Therefore, further development of the combustion wave method might lead to the widespread use of low-cost, high-speed synthesis of micro- and nanostructured materials [69].

Pyrolysis of polymers method

This method has as a carbon source a polymer or other organic compounds which undergo pyrolysis. One of the most promising pyrolysis in the production of core-shell structures is that of ferrocene. Carbon-encapsulated Fe nanoparticles with sizes between 5 and 20 nm were synthesized via a picric acid-detonation-induced pyrolysis of ferrocene, which is characterized by a self-heating and extremely fast process [83]. The formation of the core–shell nanoparticles can be selectively controlled by adjusting the composition of the picric acid-ferrocene mixture, which determines the C/Fe atomic ratio of the reaction system. This ratio of ferrocene/PA did not affect the size of the particles obtained given that in all samples the size remained the same [83].

Qiao et al. [54] described a practical and functional method for synthesizing Fe$_3$O$_4$@C core-shell, in which, initially, SiO$_2$@Fe$_3$O$_4$@C is formed using SiO$_2$ nanoparticles produced by the Stober method. Subsequently, SiO$_2$@Fe$_3$O$_4$@C is reacted with a basic solution to remove

the SiO$_2$ to form Fe$_3$O$_4$@C core–shell. The last step used by Qiao et al. [54] to produce Fe$_3$O$_4$@C core–shell was also used by Lei et al. [51], who prepared Fe$_3$O$_4$@C particles with a coaxial and penetrated hollow meso channel based on the concept of "confined nano space pyrolysis", a synthesis which involves the production of a polydopamine coating followed by a silica coating on a rod-shaped β-FeOOH nanoparticle and subsequent treatment using confined nano space pyrolysis and silica removal procedures.

Stober method

The Stober method is a particular case of sol gel process, which allows the preparation of monodispersed silica beads with sizes ranging from 5 to 2000 nm. This method is based on the hydrolysis and polycondensation of alkyl silicates in alkaline solutions of alkoxides. The main advantage of the Stober method is the ability to form mono dispersed spherical silica particles, whileacid-catalyzed systems usually result in gel structures [84,85].

Currently, the method has been modified and adapted for the synthesis of magnetic nanoparticles coated with a thin layer of silica oxide. However, there is still a limited number of works that directly describe the application of the method in the production of Core-shell of Fe$_3$O$_4$@C [50].

Zhang et al. [50] modified the Stober synthesis, which is a route specifically developed for SiO$_2$ synthesis, and succeeded in producing Fe$_3$O$_4$@C. The synthesis involves the production of a polydopamine coating followed by a silica coating on a rod-shaped β-FeOOH nanoparticle, and subsequent treatment using confined nanospace pyrolysis and silica removal procedures. Typical coaxial hollow Fe$_3$O$_4$@C possesses a rice-grain morphology and mesoporous structure with a large specific surface area, as well as a continuous and flexible carbon shell [50]. The authors also investigated some process parameters in the yield and configuration of the spheres. It was found that the yield of the Fe$_3$O$_4$@polymer is highly influenced by the concentration of ammonium hydroxide, and the mono dispersity is mainly affected by the concentration of ammonium hydroxide and the citrate group sites away from the surfaces of the Fe$_3$O$_4$ nano spheres. Interestingly, carbonization of Fe$_3$O$_4$@polymer at high temperatures makes the grain sizes of Fe$_3$O$_4$ in Fe$_3$O$_4$@C samples larger than those in the Fe$_3$O$_4$ sample, which makes the saturation magnetization value for the Fe$_3$O$_4$@C samples higher than those of commonly obtained materials [50].

Nonetheless, there are research records that use this method as one of the steps in the production of Fe$_3$O$_4$@C core-shell [86]. This method basically consists of covering the magnetite in which in situ pyrrole polymerization takes place with SiO$_2$ and pyrrole to form Fe$_3$O$_4$@SiO$_2$@ olypyrrole. Thereafter, a heat treatment is performed to form the carbon layer and subsequently removes the SiO$_2$ in basic medium [86].

Hybrids methods

The synthesis of core-shell sometimes involves the combination of various methods or hybrid methods. Therefore, some examples of "hybrid methods", which are basically the combination of several methods commonly used for the production of core-shell nanoparticles, are discussed below.

Another approach to synthesize the Fe$_3$O$_4$@C core–shell was proposed by Wu et al. [55]. This strategy is a combination of two reactions: solvothermic and hydro thermic. However, the crucial step to the formation of Fe$_3$O$_4$@C core-shell is the hydrothermic reaction

[55]. The synthesis of Fe$_3$O$_4$@C core-shell was basically carried out via polyvinylpyrrolidone-protected glucose reduction/carbonization/ Ostwald ripening. Curiously, glucose acts as a reductant and provides carbon sources to form Fe$_3$O$_4$@C nano rings. Changing the molar ratio of glucose and precursor can conveniently modulate the carbon content and the static magnetic and microwave absorption properties of the products [55].

Another method generally used to synthesize materials with higher uniformity and mono dispersity, tunable size, and high yield is the Stober method [50,52]. Similarly to other methods for obtaining Fe$_3$O$_4$@C core–shell, this method has a hydrothermal step to obtain magnetite nanoparticles. The second step is to react magnetite with formic aldehyde and resorcinol to form the Fe$_3$O$_4$@polymer. Finally, the Fe$_3$O$_4$@polymer is carbonized to obtain Fe$_3$O$_4$@C core-shell [50]. In addition, the Fe$_3$O$_4$@C obtained exhibits high uniformity and mono dispersity. Besides, Fe$_3$O$_4$@C has a magnetic susceptibility that is higher (90 emu.g^{-1}) than commonly obtained samples, which may further accelerate its magnetic separation in solution if a magnet was used [50]. This method is strongly corroborated by Tan et al. [52], who fabricated carbon shell derived from the carbonization of a resorcinol formaldehyde polymer, which possesses abundant porosity with a hierarchical structure and is highly active in the capture of aromatic sulfur and nitrogen compounds, despite the absence of any active metal sites such as Cu (I) and Ag (I).

From the many methods described in this section, the majority of those are applied in the initial stage using a hydrothermal or solvothermal reaction to generate nanoparticles Fe$_2$O$_3$ or Fe$_3$O$_4$. Other steps may involve a reaction with the polymer or with SiO$_2$ to form an intermediate and finally its carbonization or is angering with acid to form core-shells.

Application of Fe$_3$O$_4$@C Core-shell Nanoparticles in the Removal of Pollutants

Removal of dyes by Fe$_3$O$_4$@C core-shell nanoparticles

Fe$_3$O$_4$@C core-shell nanoparticles have been studied in several researches due to its applications in the adsorption of chemical species, as showed in Figure 9, which is of environmental interest. These particles are much more stable than pure magnetic particles since the shell not only protects the magnetic core of environmental degradation but also inhibits the agglomeration by Van Der Waals forces [73]. Unlike traditional adsorbent materials, Fe$_3$O$_4$@C core–shell does not require a costly step for its removal after the adsorption process, requiring only a magnetic field.

Wu et al. [17] produced magnetic Fe$_3$O$_4$@C nanoparticles by hydrothermal coprecipitation, at 160°C for 6 hrs, and applied the core-shell for the removal of methylene blue (MB) in water. Therefore, maximum adsorption capacities by adsorption kinetics, influence of pH (pH 2-12) and ionic strength in adsorption process of MB were studied. The authors observed that the pH had a significant influence on the adsorption performance of Fe$_3$O$_4$@C NPs. More MB was adsorbed at higher pH values ranging from 2-8. Wu et al. [17] attributed this behavior to the fact that at higher pH the oxygen-containing groups on Fe$_3$O$_4$@C NPs deprotonated more and interacted more strongly with MB. In the range of 8-10, the adsorption capacity of Fe$_3$O$_4$@C NPs decreased slightly. Furthermore, the influence of ionic strength was less than that of pH. When the ionic strength increased, the adsorption was inhibited. In the work above, Na$^+$ might adsorb on Fe$_3$O$_4$@C NPs as a competitor, leading to the decrease of adsorption capacity. The adsorption kinetics of MB by Fe$_3$O$_4$@C NPs showed that adsorption capacities increased

fast in the first hour and reached the equilibrium within 3 hours, which is a lower time than at 15 mg·L^{-1}. At the equilibrium concentration of 52 mg·L^{-1}, the equilibrium adsorption capacity value was 117 mg·g^{-1}.

Zhang and Kong [18] studied novel superparamagnetic Fe$_3$O$_4$@C core–shell nanoparticles for the removal of organic dyes from aqueous solutions, and the effect of pH and adsorption time in the adsorption ability. The results showed that both these parameters have influence on the adsorption process, wherein the nanoparticle showed highest adsorption capacity of 90% of MB in basic pH (7-8) and 210 min under stirring. After the adsorption is accomplished, the nanoparticles can be easily separated from the water by the application of a magnetic field. Hao et al. [19] showed that the prepared the γ-Fe$_2$O$_3$@C nano composite (20 nm) was able to remove approximately 80% of the congo red (CR) within 10 min, and the final removal efficiency of CR was up to 96.2% within 120 min. Therefore, according to the Langmuir equation, the maximum adsorption capacities of the Fe$_3$O$_4$@C and the γ-Fe$_2$O$_3$@C nano composites for CR were calculated to be 48.1 and 105.3 mg·g^{-1}, respectively.

Zhang et al. [87] synthesized Fe$_3$O$_4$@C NPs by using citrus pectin as the carbon source. The as-prepared nanoparticles were spherical, with the smallest uniform size of 7 nm among all reported and large specific surface area. Surprisingly, the Fe$_3$O$_4$@C NPs further demonstrated dramatic ability to remove methylene blue for a maximum adsorption capacity of 141.3 mg·g^{-1} and superior recyclability (up to 20 cycles). Further experimental results revealed that the adsorption kinetic and isotherm fitted well with the pseudo-second-order kinetic and Freundlich isotherm model, respectively.

Lin et al. [12] showed that Fe$_3$O$_4$@C nanoparticles with mesoporous carbon are efficient nano adsorbents, and that rhodamine B (RhB) concentrations decreased with the increase in adsorption time. Therefore, magnetic core–shell Fe$_3$O$_4$@nSiO$_2$@mSiO$_2$ nanoparticles were first synthesized with polyethylene glycol as a template in acid conditions, which possesses high BET surface area and large pore volume. Then Fe$_3$O$_4$@nSiO$_2$@mSiO$_2$ nanoparticles were used as hard templates to synthesize Fe$_3$O$_4$@mesoporous carbon (Fe$_3$O$_4$@C) with large surface area (971 m^2·g^{-1}) and pore volume (1.4 cm^3·g^{-1}). The high surface area and mesoporous structure of Fe$_3$O$_4$@C favor its efficient adsorption of RhB in aqueous solution, exhibiting an adsorption capacity of 198.9 mg·g^{-1} within 30 min, which is higher than the previous reports on magnetic mesoporous graphitic carbon and magnetic mesoporous resin. More noticeably, Fe$_3$O$_4$@C nanoparticles displayed super paramagnetic property, which allows them to be easily separated and collected in real-life applications.

Zhou and Liu [28] compared adsorption capacities of cationic and anionic dyes Fe$_3$O$_4$@polydopamine (PDA) and derived Fe$_3$O$_4$@carbon core–shell nanoparticles. The study demonstrates that Fe$_3$O$_4$@PDA and Fe$_3$O$_4$@C, both with average size of 300 nm, show different adsorption behavior towards two kinds of organic dyes. The surface charge of adsorbents plays a critical effect on the adsorption performance. The electrostatic interaction is believed to determine the selective adsorption behavior of Fe$_3$O$_4$@PDA and Fe$_3$O$_4$@C NPs for cationic and anionic dyes. The results indicate that the negatively charged Fe$_3$O$_4$@ PDA NPs have higher adsorption capacity for positive charged MB, while positively charged Fe$_3$O$_4$@C NPs exhibit better performance for negative charged MO, which strongly suggests that the interaction between adsorbent and adsorbate is electrostatic. In summary, the different adsorption behavior together with the magnetic separation provide a simple and versatile strategy toward designing hybrid NPs for a variety of requirements in water pollution treatment.

Removal of pharmaceuticals by Fe$_3$O$_4$@C core-shell nanoparticles

Although pharmaceuticals have been present in water for decades, their levels in the environment have only recently begun to be quantified and acknowledged as potentially hazardous to ecosystems [3]. Some pollutants groups have received special attention since the late 90s [4], due to correlations between the development and rapid expansion of antibiotic resistance and their total consumption and occurrence in the environment [4,5]. According to Bartlett et al. [88], the resistance within all microbial classes continues to grow by a natural evolution driven by the massive use of agents that apply selective antimicrobial pressure, and pharmaceutical development that had previously kept men ahead of resistance is now stalled due to economic and regulatory barriers.

Antibiotics have been investigated as sources of water contaminants, possibly affecting surface water and groundwater [16,89]. To solve this problem, adsorption methods are used, since they are considered as an effective way to remove antibiotics from water [90]. To this end, studies have shown that core-shell nanoparticles and magnetic nanostructures can be effective in the adsorption of different antibiotics, such as sulfonamide [15], nafcillin [91] and tetracycline [92].

The drug (antibiotics) adsorption by core-shell nanoparticles is sensitive to different factors, such as pH, ionic strength, concentration and chemical structure of drugs [92]. Bao et al. [15], for instance, showed that nano composite Fe$_3$O$_4$@C (Fe$_3$O$_4$ coated with carbon) exhibited a high adsorption affinity for sulfonamides (a type of antibiotic) and that the adsorption is pH-dependent [15]. The maximum adsorption, obtained at pH 4.8, was 96%, decreasing at pH from 6 to 9 or at pH 2.3 [15]. On the other hand, Wang et al. [93] showed that the adsorption ability of chlortetracycline (tetracycline antibiotic) from water by magnetic carbon nanoparticles with core-shell structure increased with solution pH at pH 3.5-7.5, but decreased with further increase of pH (pH 7.5-8.5). Furthermore, Bao et al. [15] also showed that there is a difference in the adsorption capacity of the antibiotics due to their chemical structure. Among sulfathiazole, sulfamethoxazole, sulfamethizole, sulfadimethoxine and sulfamethazine, sulfathiazole was the one with the highest affinity to be adsorbed by the core-shell structure, probably because of the minimum steric hindrance of the thiazole ring of this antibiotic [15].

In addition to the factors already discussed, the contact time between the antibiotic or drug with the core-shell nanoparticle can also affect the adsorptive capacity. Some antibiotics, when contacted with core-shell structures, such as sulfonamide, exhibit rapid adsorption kinetics from 90-200 s to reach adsorption equilibrium and high adsorption capacity (Qmax=344.8 µg g^{-1}) [94]. Differently, the adsorption of tetracycline in aqueous solutions by magnetic composites of Fe$_3$O$_4$@C takes about 44 min to adsorb 79% [32]. In another study it was observed that the core–shell titanium dicarboxylate with indium (III) sulfide (In$_2$S$_3$@MIL-125(Ti) hybrids shows good adsorption, and the adsorption amount of tetracycline was 119.2 mg·g^{-1} after 300 min [92].

All these factors and characteristics influence the percentage of adsorbed drugs from water resources and also affect the mechanism with core-shell nanoparticles. Some studies indicate that hydrogen bonding, electrostatic interactions and electron-donor-acceptor interactions were the major forces for core-shell adsorption [15,92]. However, each reaction will have its peculiarities and an in-depth study for each specific case will be indispensable for the proper identification of the mechanism involved in the process.

Removal of heavy metals by Fe$_3$O$_4$@C core-shell nanoparticles

With the rapid development of industries, such as metal plating facilities, mining operations, fertilizer industries, tanneries, batteries, paper industries and pesticides, etc., heavy metal containing wastewater are increasingly directly or indirectly discharged into the environment [95]. Thus, due to the adverse effects on environmental and human health caused by toxic metal ions, some technologies are applied for the decontamination of heavy metals such as reverse osmosis, precipitation and adsorption. The advantage of the latter is its low cost and its high treatment speed [6]. To remove heavy metals, carbon nano materials have also been associated with other magnetic nanoparticles, presenting promising results [6,34,82,96].

Zhao et al. [6] prepared, applied and recycled Fe$_3$O$_4$@C NPs for the removal of Cu^{2+}. The mixture of FeCl$_2$-4H$_2$O and FeCl$_3$-6H$_2$O was submitted to a hydrothermal treatment at a temperature of 160°C for 6 hrs. In this adsorption isotherm study, the copper was selected because its toxicity is known. Then, 8,0 mL of Cu^{2+}, ph 5, 6.4-35.2 mg·L^{-1}, with solubility lower than 91.8 g·L^{-1} were added to 5 mg of Fe$_3$O$_4$@C NPs in a thermostatic shaker at 35°C for 24 h to reach saturation. In that study the adsorption capacity increased notably in values of equilibrium concentration lower than 0.04 mg·L^{-1}, while above this value the adsorption capacity increased moderately. In the value of equilibrium concentration of 1.0 mg·L^{-1}, the value of equilibrium adsorption capacity reached 54.7 mg·L^{-1}. This value of equilibrium concentration was adopted as reference, since the Environmental Protection Agency of the United States use the same amount as the recommended value of Cu for drinking water. The study showed a Fe$_3$O$_4$@C NPs adsorption capacity 10 times higher than that of active carbon. The next step consisted of magnetic separation, which decreased less than 2.5% after its fourth cycle.

Zare et al. [97] synthesized nanoparticles of Fe$_3$O$_4$ as an adsorbent for rapid removal of ammonium ion from the solvent phase. The Fe$_3$O$_4$ NPs were obtained by the chemical coprecipitation method from the mixtures of FeCl$_2$·4H$_2$O and FeCl$_3$·6H$_2$O with the addiction of HCl. This solution was stirred at 30°C at a constant pH of 9 for 1 h and the precipitate was mixed at 50°C for 30 min. With this process a particle size of 6 nm was obtained. The study investigated the effect of contact time (10 to 80 min), pH (1 to 10), temperature (25 to 75°C) and initial concentration of ammonium ions (80 to 140 mg·L^{-1}) in the adsorption capacity of ammonium ion by Fe$_3$O$_4$ nanoparticles. The values of the optimized parameters were found to be 40 min, pH 10, 25°C and 140 mg·L^{-1} of ammonium ions, respectively. Among these parameters, the pH was presented as the most influential factor in increasing adsorption, since the percentage of ammonium removal by Fe$_3$O$_4$ NPs increased from to 21.25% to 93.12% in accordance to the increase of pH until 10. This result corroborates the study by Sadegh et al. [98], which claims the pH is one of the most important factors in adsorption capacity.

In their adsorption study Zare et al. [97] used a flask with 10 mL of ammonium ion solution with an initial concentration of 140 mg·L^{-1}and 0.05 g of adsorbent. To optimize the adsorption process the authors established the most appropriate correlation coefficient for the equilibrium curves using the following isotherms equations: Langmuir, Freundlich, Temkin, and Harkins–Jura. Langmuir model successfully described the adsorption of ammonium ions onto Fe$_3$O$_4$.

Zare et al. [97] investigated three models to describe the mechanism of solute adsorption by a sorbent: pseudo-first order equation of Lagergren, pseudo-second order and intra particle diffusion model. The model that better describes acorrelation was the pseudo-second.

Zhang et al. [99] synthesized mesoporous magnetic Fe$_3$O$_4$@C nano spheres by hydrothermal coprecipitation, at 200°C for 24 h, and studied the influence of core-shell nano spheres comparing them with magnetic Fe$_3$O$_4$ nano spheres for the removal of Cr (IV) from water. Cr (IV) removal experiments were carried out by adsorbing Cr (IV) from aqueous solutions at 28°C and pH 7.6. Firstly, the nano spheres were dispersed in the Cr (IV) solution; then, after 150 min, the magnetic materials were attracted and separated by an external magnet. The authors concluded that Fe$_3$O$_4$@C nano spheres with an average pore size of 6.2 nm removed more Cr (IV) when compared with magnetic Fe$_3$O$_4$ nano spheres, reaching 92.4%.

Conclusions

Fe$_3$O$_4$@C core-shell nanoparticles are used in environmental remediation for water pollution issues as well as for protecting human health from exposure to harmful materials, such as dyes, pharmaceuticals, oils, heavy metals, etc. These nanoparticles have a high adsorption capacity and facilitated separation due to magnetic characteristics. These properties make Fe$_3$O$_4$@C core-shell nanoparticles a potential material for use in the treatment of wastewater.

Financial Support

References

1. Lingling Q, Tingting H, Zhijun L, Canca L, Yan M, et al. (2015) One-step fabricated Fe$_3$O$_4$@C core-shell composites for dye removal: kinetics, equilibrium and thermodynamics. Journal of Physics and Chemistry of Solids 78: 20-27.

2. Mahmoodi MN, Abdi J, Bastani D (2014) Direct dyes removal using modified magnetic ferrite nanoparticle. J Environ Health Sci Eng 12: 96.

3. Rivera-Utrilla J, Sanchez-Polo M, Ferro-Garcia MA, Prados-Joya G, Ocampo-Perez R (2013) Pharmaceuticals as emerging contaminates and their removal from water: A review. Chemosphere 93: 1268-1287.

4. Carvalho IT, Santos L (2016) Antibiotics in the aquatic environments: A review of the European scenario. Environment International 94: 736-757.

5. Krummerer K (2001) Drugs in the environment: emission of drugs, diagnostic aids and disinfectants into wastewater by hospital in relation to other sources- a review. Chemosphere 45: 957-969.

6. Zhao L, Chang v, Liao R, Zhang X, Xie J, et al. (2014) Facile hydrothermal preparation of S-doped Fe$_3$O$_4$@C nanoparticles for Cu^{2+} removal. Material letters 135: 154-157.

7. Duodu GO, Goonetilleke A, Ayoko GA (2016) Comparison of pollution indices for the assessment of heavy metal in Brisbane River sediment. Environmental Pollution 219: 1077-1091.

8. Nethaji S, Ralaivanan R, Viswam A, Jayaprakash M (2017) Geochemical assessment of heavy metals pollution in surface sediments of Velar and Celeron estuaries southeast coast of India. Marine Pollution Bulletin 115: 469-479.

9. Zhang M, Liu GH, Cancao K, Wang Z, Zhao Q, et al. (2015) Biological treatment of 2, 4, 6-trinitrotoluene (TNT) red water by immobilized anaerobic-aerobic microbial filters. Chemical Engineering Journal 259: 876-884.

10. Weiyi W, Zhao-Hong H, Teik-Thye L (2014) Recent development of mixed metal oxide anodes for electrochemical oxidation of organic pollutants in water. Applied Catalysis A: General 480: 58-78.

11. Pastrana-Martínez LM, Morales-Torres S, Figueiredo JL, Faria JL, Silva AM (2015) Graphene oxide based ultrafiltration membranes for photo catalytic degradation of organic pollutants in salty water. Water Research 77: 179-190.

12. Lin L, Qiancheng Z, Tongbao W, Fangxiao W, Jun M, et al. (2014) The synthesis of core-shell Fe$_3$O$_4$@mesoporous carbon in acidic medium its efficient removal of dye. Micro porous and Mesoporous Materials 197: 221-228.

13. Yanming S, Lincheng Z, Chao B, Junjun M, Mingzhu L, et al. (2016) Magnetic responsive metal-organic frameworks nano sphere with core-shell structure for highly efficient removal of methylene blue. Chemical Engineering Journal 283: 1127-1136.

14. Yu K, Ho J, McCandlish E, Buckley B, Patel R, et al. (2013) Cooper ion adsorption by chitosan nanoparticles and alginate micro particles for water purification applications. Colloids and Surfaces Physico chem Eng Aspects 425: 31-41.

15. Bao X, Qiang Z, Chang JH, Ben W, Qu J (2014) Synthesis of carbon-coated magnetic nano composite (Fe$_3$O$_4$@C) and its application for sulfonamide antibiotics removal from water. Journal of Environmental Sciences 26: 962-969.

16. Zhang B, Zhang H, Li X, Lei X, Li C, et al. (2013) Synthesis of BSA/Fe$_3$O$_4$ magnetic composite microspheres for adsorption of antibiotics. Materials Science and Engineering 33: 4401-4408.

17. Wu R, Liu JH, Zhao L, Zhang X, Xie J, et al. (2014) Hydrothermal preparation of magnetic Fe$_3$O$_4$@C nanoparticles for dye adsorption. Journal of Environmental Chemical Engineering 2: 907-913.

18. Zhang Z, Kong J, Novel J (2011) magnetic Fe$_3$O$_4$@C nanoparticles as adsorbents for removal of organic dyes from aqueous solution. Journal of Hazardous Materials 193: 325-329.

19. Hao T, Rao X, Li Z, Niu C, Su X (2014) Synthesis of magnetic separable iron oxide/carbon nano composites for efficient adsorptive removal of congo red. Journal of Alloys and Compounds 617: 76-80.

20. Maryam F, Ghanei-Motlagh M, Taher MA (2015) The adsorption of basic dye (Alizarin red S) from aqueous solution onto activated carbon/y-Fe$_2$O$_3$ nano-composite: Kinetic and equilibrium studies. Material Science in Semiconductor Processing 40: 35-43.

21. Jauris IM, Faga SB, Adebayo MA, Machado FM (2016) Adsorption of acridine Orange and methylene blue synthetic dyes and anthracene on single wall carbon nanotubes: a first principle approach. Computational and Theoretical Chemistry 1076: 42-50.

22. Ganpupomu RH, Sattler ML, Ramirez D (2016) Comparative study of carbon nanotubes and granular activated carbon: physicochemical properties and adsorption capacities. Journal of Hazardous Materials 302: 362-374.

23. Ihsanullah AA, Al-Amer AM, Laoui T, Al-Marri MJ, Nasser MS, et al. (2016) Heavy metal removal from aqueous solution by advanced carbon nanotubes: Critical review of adsorption applications. Separation and Purification Technology 157: 141-161.

24. Yeganegi S, Gholampour F (2016) Simulation of methane adsorption and diffusion in a carbon nanotube channel. Chemical Engineering Science 140: 62-70.

25. Blaney L (2007) Magnetite (Fe$_3$O$_4$): Properties, Synthesis, and Applications, Lehigh University Lehigh Preserve, USA 15: 2007.

26. Fan H, Li B, Feng Y, Qiu D, Song Y (2016) Multifunctional Fe$_3$O$_4$@SiO$_2$@GdVO4:Eu3þ core-shell nano composite for a potential drug Carrier. Ceramics International 42: 13326-13330.

27. Serenjeh FN, Hashemi P, Rasoolzadeh F (2015) A simple method for the preparation of spherical core-shell nano magnetic agarose particles. Colloids and Surfaces A: Physico chem Eng Aspects 465: 47-53.

28. Zhou Z, Liu R (2017) Fe$_3$O$_4$@polydopamine and derived Fe$_3$O$_4$@carbon core–shell nanoparticles: Comparison in adsorption for cationic and anionic dyes. Colloids and Surfaces A: Physico chem Eng Aspects 522: 260-265.

29. Xiao F, Feng C, Jin C, Liu X, Pan L, et al. (2014) Magnetic and electromagnetic properties of Fe$_3$O$_4$/C self-assemblies. Materials Letters 122: 103-105.

30. Kakavandi B, Kalantary RR, Jafari AJ, Nasseri S, Ameri A, et al. (2015) Pb(II) adsorption onto a magnetic composite of activated carbon and super paramagnetic Fe$_3$O$_4$ nanoparticles: experimental and modeling study. CLEAN-Soil, Air, Water 43: 1157-1166.

31. Shi D, Yang H, Ji S, Jiang S, Liu v, et al. (2015) Preparation and characterization of core-shell structure Fe$_3$O$_4$@C magnetic nanoparticles. Procedia Engineering 102: 1555-1562.

32. Kakavandi B, Takdastan A, Jaafarzadeh N, Azizi M, Mirzaei A, et al. (2016) Application of Fe$_3$O$_4$@C catalyzing heterogeneous UV-Fenton system for tetracycline removal with a focus on optimization by response surface method. Journal of Photochemistry and Photobiology a: Chemistry 314: 178-188.

33. Luo H, Huang K, Sun B, Zhong J (2014) Strategy to Synthesize Fe$_3$O$_4$/C Nanotubes as Anode Material for Advanced Lithium-Ion Batteries. Electro chimica Acta 149: 11-17.

34. Xuan S, Hao L, Jiang W, Gong X, Hu Y, et al. (2007) A facile method to fabricate carbon-encapsulated Fe$_3$O$_4$ core/shell composites. Nanotechnology 18: 035602.

35. Yang F, Su H, Zhu Y, Chen J, Lau WM, et al. (2013) Bio inspired synthesis and gas-sensing performance of porous hierarchical α-Fe₂O₃/C nano composites. Scripta Materialia 68: 873-876.

36. Xue XY, Ma CH, Cui CX, Xing LL (2011) High lithium storage performance of a-Fe₂O₃/graphene nano composites as lithium-ion battery anodes. Solid State Sciences 13: 1526-1530.

37. Chen YJ, Xiao G, Wang TS, Ouyang OY, Qi LH, et al. (2011) Porous Fe₃O₄/ Carbon Core/Shell Nanorods: Synthesis and Electromagnetic Properties. J Phys Chem 115: 3603-13608.

38. Li P, Deng J, Li Y, Liang W, Wang K, et al. (2014) One-step solution combustion synthesis of Fe₂O₃/C nano-composites as anode materials for lithium ion batteries. Journal of Alloys and Compounds 590: 318-323.

39. Luo P, Yu J, Shi Z, Wang F, Liu L, et al. (2012) Fabrication and super capacitive properties of Fe₂O₃@C nano composites. Materials Letters 80: 121-123.

40. Zhou J, He J, Wang T, Li G, Guo Y, et al. (2011) Design of meso structured γ-Fe₂O₃/carbon nano composites for electromagnetic wave absorption applications. Journal of Alloys and Compounds 509: 8211-8214.

41. Bhattacharya K, Gogoi B, Buragohain AK, Deb P (2014) Fe₂O₃@C nano composites having distinctive antioxidant activity and hemolysis prevention efficiency. Materials Science and Engineering 42: 5965-600.

42. Ambashta RD, Sillanpaa M (2010) Water purification using magnetic assistance: A review. Journal of Hazardous Materials 180: 38-49.

43. Hay AT (1873) Improvement in electrical protection for boilers. US Patent 140: 196.

44. Eichholz C, Knool J, Lerche D, Nirschl H (2014) Investigations on the magnetization behavior of magnetic composite particles. Journal of Magnetism and Magnetic Materials 368: 139-148.

45. Shouhu X, Lingyun H, Wanquan J, Xinglong G, Yuan H, et al. (2007) A facile method to fabricate carbon-encapsulated Fe₃O₄ core/shell composites. Nano technology pp: 18: 3.

46. Zhihang Z, Yanbao L, Song Y, Haichen Y (2016) Preparation of calcium carbonate@graphene oxide core-shell microspheres in ethylene glycol for drug delivery. Ceramics International 42: 2281-2288.

47. Zhao Y, Li J, Wu C, Ding Y, Guan L (2012) A Yolk-Shell Fe₃O₄@C Composite as an Anode Material for High-Rate Lithium Batteries. Chem Plus Chem 77: 748-751.

48. Jin YH, Seo S, Shim HW, Park KS, Kim DW (2012) Synthesis of core/shell spinel ferrite/carbon nanoparticles with enhanced cycling stability for lithium ion battery anodes. Nanotechnology 23: 125402.

49. Zheng J, Liu ZQ, Zhao XS, Liu M, Liu X, et al. (2012) One-step solvothermal synthesis of Fe₃O₄@ C core–shell nanoparticles with tunable sizes. Nanotechnology 23: 165601.

50. Zhang XB, Tong HW, Liu SM, Yong GP, Guan YF (2013) An improved Stober method towards uniform and mono disperse Fe₃O₄@C nano spheres. Journal of Materials Chemistry 25: 7488-7493.

51. Lei C, Han F, Sun Q, Li WC, Lu AH (2014) Confined Nano space Pyrolysis for the Fabrication of Coaxial Fe₃O₄@ C Hollow Particles with a Penetrated Meso channel as a Superior Anode for Li-Ion Batteries. Chemistry A European Journal 20: 139-145.

52. Tan P, Jiang Y, Liu X, Zhang DY, Sun LB (2016) Magnetically Responsive Core-Shell Fe₃O₄@C Adsorbents for Efficient Capture of Aromatic Sulfur and Nitrogen Compounds. ACS Sustainable Chemistry and Engineering 4: 2223-2231.

53. Wang L, Gan K, Lu D, Zhang J (2016) Hydrophilic Fe₃O₄@C for High-Capacity Adsorption of 2, 4-Dichlorophenol. European Journal of Inorganic Chemistry 6: 890-896.

54. Qiao X, Sun A, Wang C, Chu C, Ma S, et al. (2016) Electric field induced structural color changes of highly mono disperse hollow Fe₃O₄@C colloidal suspensions. Colloids and Surfaces A: Physicochemical and Engineering Aspects 498: 74-80.

55. Wu T, Liu Y, Zeng X, Cui T, Zhao Y, et al. (2016) Facile Hydrothermal Synthesis of Fe₃O₄/C Core–Shell Nano rings for Efficient Low-Frequency Microwave Absorption. ACS applied materials and interfaces 11: 7370-7380.

56. Cunningham A, Bürgi T (2013) Amorphous Nano photonics: Bottom-up Organisation of Metallic Nanoparticles. Springer Berlin Heidelberg P: 1-37.

57. Chaudhuri RG, Paria S (2012) Core/Shell nanoparticles: classes, properties, synthesis mechanisms, characterizations, and applications. Chemical Reviews 112: 2373-2433.

58. Martiradonna L, Qualtieri A, Stomeo T, Carbone L, Cingolani R, et al. (2007) Lithographic nano-patterning of colloidal nano crystal emitters for the fabrication of waveguide photonic devices. Sensors and Actuators B: Chemical 126: 116-119.

59. Ruffino F, Maugeri P, Cacciato G, Zimbone M, Grimaldi MG (2016) Metal nanostructures with complex surface morphology: The case of supported lumpy Pd and Pt nanoparticles produced by laser processing of metal films. Physica E: Low-dimensional Systems and Nanostructures 83: 215-226.

60. Li Y, Scott J, Chen YT, Guo L, Zhao M, et al. (2015) Direct dry-grinding synthesis of monodisperse lipophilic CuS nanoparticles. Materials Chemistry and Physics 162: 671-676.

61. Moonngam S, Tunijina P, Deesom D, Banjongprasert C (2016) Fe-Cr/CNTs nano composite feedstock powders produced by chemical vapor deposition for thermal spray coatings. Surface and Coatings Technology 306: 323-327.

62. Panov MS, Tumkin II, Smikhovskaia AV, Khairullina EM, Gordeychuk DL, et al. (2016) High rate in situ laser-induced synthesis of copper nanostructures performed from solutions containing potassium bromate and ethanol. Microelectronic Engineering 157: 13-18.

63. Luesakul U, Komenek S, Puthong S, Muangsin N (2016) Shape-controlled synthesis of cubic-like selenium nanoparticles via the self-assembly method. Carbohydrate Polymers 153: 435-444.

64. Pomelova TA, Khandarkhaeva SE, Podlipskaya TY, Naumov NG (2016) Top-down synthesis and characterization of exfoliated layered KLnS₂ (Ln = La, Ce, Gd, Yb, Lu) nano sheets, their colloidal dispersions and films. Colloids and Surfaces A: Physicochemical and Engineering Aspects 504: 298-304.

65. Laurent S, Forge D, Port M, Roch A, Robic C, et al. (2008) Magnetic Iron Oxide Nanoparticles: Synthesis, Stabilization, Vectorization, Physicochemical Characterizations, and Biological Applications. Chem 108: 2064-2110.

66. Lai L, Xie Q, Chi L, Gu W, Wu D (2016) Adsorption of phosphate from water by easily separable Fe₃O₄@SiO₂ core/shell magnetic nanoparticles functionalized with hydrous lanthanum oxide. Journal of Colloid and Interface Science 465: 76-82.

67. Zhou Q, Wang Y, Xiao J, Fan H (2016) Adsorption and removal of bis phenol A, a-naphthol and b-naphthol from aqueous solution by Fe₃O₄@polyaniline core-shell nano materials. Synthetic Metals 212: 113-122.

68. Xiao G, Su H, Tan T (2015) Synthesis of core–shell bio affinity chitosan– TiO₂ composite and its environmental applications. Journal of Hazardous Materials 283: 888-896.

69. Shin J, Lee LK, Yeo T, Choi W (2016) Facile One-pot Transformation of Iron Oxides from Fe₂O₃ Nanoparticles to Nanostructured Fe₃O₄@C Core-Shell Composites via Combustion Waves. Scientific Reports.

70. Byrappa K, Adschiri T (2007) Hydrothermal technology for nanotechnology. Prog Cryst Growth Charact 53: 117-166.

71. Gribanov NM, Bibik EE, Buzunov OV, Naumov VN (1990) Physico-chemical regularities of obtaining highly dispersed magnetite by the method of chemical condensation. Journal of Magnetism and Magnetic Materials 85: 7-10.

72. Li L, Wang T, Zhang L, Su Z, Wang C, et al. (2012) Selected-Control Synthesis of Monodisperse Fe₃O₄@C Core–Shell Spheres, Chains, and Rings as High-Performance Anode Materials for Lithium-Ion Batteries. Chem Eur J 18: 36.

73. Wang Z, Xiao P, He N (2006) Synthesis and characteristics of carbon encapsulated magnetic nanoparticles produced by a hydrothermal reaction. Carbon 44: 3277-3284.

74. Gersten B (2005) Solvothermal synthesis of nanoparticles. Chem Files 5: 11-12.

75. Hou S, Chi Y, Zhao Z (2017) Synthesis of core-shell structured magnetic nanoparticles with a carbide shell, In IOP Conference Series. Materials Science and Engineering 182: 012026.

76. Li M, Cao Y, Ni X, Cao G (2017) Rapid Evaporation-Induced Self-assembly of Three-Dimensional Photonic Crystals Using Fe₃O₄@C Magnetic Nano composites. New J Chem 41: 1980-1985.

77. Melinon P, Begin-Colin S, Duvail JC, Gaure F, Herlin-Boime N (2014) Engineered inorganic core/shell nanoparticles. Physics Reports Elsevier 543: 163-197.

78. Srdic VV, Mojic B, Nikolic M, Ognjanovic S (2013) Recent progress on synthesis of ceramics core/shell nanostructures, Processing and Application of Ceramics 7: 45-62.

79. Wang B, Wang G, Zheng Z, Wang ZH, Bai J, et al. (2013) Carbon coated Fe₃O₄ hybrid material prepared by chemical vapor deposition for high performance lithium-ion batteries. Electro chimica Acta 106: 235-243.

80. Zhu Q, Tao F, Pan Q (2010) Fast and selective removal of oils from water surface via highly hydrophobic core-shell Fe₂O₃@C nanoparticles under magnetic field. Appl Mater Interfaces 2: 3141-3146.

81. Zhu J, Pallavkar S, Chen M, Yerra N, Luo Z, et al. (2013) Magnetic carbon nanostructures: microwave energy-assisted pyrolysis vs. Conventional pyrolysis. Chem Commun 49: 258.

82. Wang J, Gao M, Wang D, Li X, Dou Y, et al. (2015) Chemical vapor deposition prepared bi-morphological carbon-coated Fe₃O₄ composites as anode materials for lithium-ion batteries. Journal of Power Sources 282: 257-264.

83. Lu Y, Zhenping Z, Zhenyu L (2005) Carbon-encapsulated Fe nanoparticles from detonation-induced pyrolysis of ferrocene. Carbon 43: 369-374.

84. Stober W, Fink A, Bohn E (1968) Controlled growth of monodisperse silica spheres in the micron size range. Journal of colloid and interface science 26: 62-69.

85. Wong YJ, Zhu L, Teo WS, Tan YW, Yang Y, et al. (2011) Revisiting the stober method inhomogeneity in silica shells. Journal of the American Chemical Society 133: 11422-11425.

86. Tian C, Du Y, Cui C, Deng Z, Xue J, et al. (2017) Synthesis and microwave absorption enhancement of yolk–shell Fe₃O₄@ C microspheres. Journal of Materials Science 52: 6349-6361.

87. Zhang W, Zhang LY, Zhao XY, Zhou Z (2016) Citrus pectin derived ultrasmall Fe₃O₄@C nanoparticles as a high-performance adsorbent toward removal of methylene blue. Journal of Molecular Liquids 222: 995-1002.

88. Bartlett JG, Gilbert DN, Spellberg B (2013) Seven ways to preserve the miracle of antibiotics. Clin Infect Dis 56: 1445-1450.

89. Shi L, Ma F, Han Y, Zhang X, Yu H (2014) Removal of sulfonamide antibiotics by oriented immobilized laccase on Fe₃O₄ nanoparticles with natural mediators. Journal of Hazardous Materials 279: 203-211.

90. Wang T, Pan X, Bem W, Wang J, Hou P, et al. (2016) Adsorptive removal of antibiotics from water using magnetic ion exchange resin. Journal of Environmental Sciences 52: 111-117.

91. Chen L, Liu Y, He X, Zhang Y (2015) Preparation and characterization of core-shell structural magnetic molecularly imprinted polymers for nafcillin. Chinese journal of chromatography 33: 481-487.

92. Wang H, Yuan X, Wu Y, Zeng G, Dong H, et al. (2016b) In situ synthesis of In₂S₃@MIL-125 (Ti) core–shell micro particle for the removal of tetracycline from wastewater by integrated adsorption and visible-light-driven photo catalysis. Applied Catalysis B: Environmental 186: 19-29.

93. Wang YX, Zhang D, Niu HY, Meng ZF, Cai YQ (2012) Synthesis of Core/Shell Structured Magnetic Carbon Nanoparticles and Its Adsorption Ability to Chlortetracycline in Aquatic Environment. College of Science 33: 1234-1240.

94. Kong X, Gao R, He X, Chen L, Zhang Y (2012) Synthesis and characterization of the core–shell magnetic molecularly imprinted polymers (Fe₃O₄@MIPs) adsorbents for effective extraction and determination of sulfonamides in the poultry feed. Journal of Chromatography A 1245: 8-16.

95. Thatai S, Khurana P, Boken J, Prasad S, Kumar D (2014) Nanoparticles and core-shell nano composite based new generation water remediation materials and analytical techniques: A review. Micro chemical Journal 116: 62-76.

96. Xie G, Xi P, Liu H, Chen F, Huang L, et al. (2012) A facile chemical method to produce super paramagnetic grapheneoxide-Fe₃O₄ hybrid composite and its application in the removal of dyes from aqueous solution. Journal of Material Chemistry 22: 1033-1039.

97. Zare K, Sadegh H, Shahryari-Ghoshekandi R, Asif M, Tyagi I, et al. (2016) Equilibrium and kinetic study of ammonium ion adsorption by Fe₃O₄ nanoparticles from aqueous solutions. Journal of Molecular Liquids 213: 345-350.

98. Sadegh H, Shahryari-ghoshekandi R, Tyagi I, Agarwal S, Gupta VK (2015) Kinetic and thermodynamic studies for alizarin removal from liquid phase using poly-2-hydroxyethyl methacrylate (PHEMA). Journal of Molecular Liquids 207: 21-27.

99. Zhang H, Liu DL, Zeng LL, Li M (2013c) ß-Cyclo dextrin assisted one-pot synthesis of mesoporous magnetic Fe₃O₄@C and their excellent performance for the removal of Cr (VI) from aqueous solutions. Chinese Chemical Letters 24: 341-343.